Tellus (1990), *42B*, 272–284

The effects of microphysical parameterization on model predictions of sulfate production in clouds

By DEAN A. HEGG[1] and TIMOTHY V. LARSON[2], [1]*Department of Atmospheric Sciences;* [2]*Department of Civil Engineering, University of Washington, Seattle, WA 98195, USA*

(Manuscript received 25 October 1988; in final form 4 July 1989)

ABSTRACT

Model predictions of sulfate production by an explicit cloud chemistry parameterization are compared with corresponding predictions by a bulk chemistry model. Under conditions of high SO_2 and H_2O_2, the various model predictions are in reasonable agreement. For conditions of low H_2O_2, the explicit microphysical model predicts sulfate production as much as 30 times higher than the bulk model, though more commonly the difference is of the order of a factor of 3. The differences arise because of the size-dependent distribution of pH in the droplets, which is in turn a consequence of the size-dependent distributions of sulfate and ammonium ions. Experimental evidence for differing size-dependent distributions of ammonium and sulfate ions is reviewed and compared with model predictions. The results of the sulfate production comparison suggest that bulk cloud water pH is not always a reliable indicator of aqueous reaction conditions in clouds. Related to this, the ozone oxidation of aqueous S(IV) appears to be of more significance than would be suggested by pH measurements of bulk cloud water.

1. Introduction

It is now widely accepted that clouds play an important role in the chemical cycles of a number of trace constituents in the troposphere (NRC, 1984). In particular, sulfur and nitrogen species are generally held to interact extensively with cloud hydrometeors. Consequently, the number of modeling studies of cloud chemistry (both prognostic and diagnostic) has increased dramatically in the last few years (e.g., Easter and Hales, 1983; Chameides, 1984; Hegg et al., 1984; Trembley and Leighton, 1984; Lee and Shannon, 1985; Flossman et al., 1985, 1987). The complexities of the processes involved have discouraged investigators from simultaneously modeling all aspects of cloud chemistry and cloud physics with equal rigor. For example, in the Long Range Transport models (LRT's) commonly employed to address such issues as acid deposition, only a "bulk" type parameterization is generally feasible. For computational simplicity, the widely-used bulk model treats the droplet spectrum as a single, well-mixed, ideal solution droplet that maintains vapor-liquid equilibrium with surrounding trace gases. In this paper, we discuss the tradeoff between accuracy and computational simplicity implicit in such assumptions by examining how much these assumptions affect the bulk model's prediction of sulfate formation in cloud droplets. We consider primarily the process of sulfate formation because previous theoretical (Howell, 1949; Hegg and Hobbs, 1979) and experimental (Noone et al., 1988) results indicate that pH (and therefore the SO_2 oxidation rate) varies across the droplet spectrum and that this, in turn, may affect the overall sulfate production rate in the cloud. Our approach is to compare the predictions of sulfate production from a bulk model to those of a more explicit model. In the course of this comparison, other interesting facets of cloud chemistry attributable to the polydisperse nature of the reaction medium will arise and will be discussed.

2. The cloud models

In order to distinguish the effects of bulk parameterization from the effects of the approximations inherent in cloud chemistry models, the models employed in this study were kept as dynamically simple as possible. Both the bulk and explicit microphysical models are Lagrangian adiabatic parcel models. For purposes of comparability, the models will be kinematic, i.e., the vertical velocity profile will be initially specified. Two different profiles will be employed, one representative of convective and one of stratiform clouds. The convective profile utilized is taken from the study of Mason and Chien (1962) and is typical of moderate cumulus (maximum undraft of 3 m s^{-1}). The stratiform profile is simply a constant updraft of 50 cm s^{-1}. These parcel models, both explicit and bulk, are essentially equivalent to cloud chemical models which have been widely employed in previous studies (e.g., Hong and Carmichael, 1983; Jacob and Hoffman, 1983; Hegg and Hobbs, 1986; and Hough, 1987). Indeed, the bulk model is very similar to the "cumulus modules" employed in many Eulerian acid deposition models (e.g., Venkatram and Karamchandari, 1986).

Both types of model have a single hydrometer phase (liquid water). The use of a single-phase cloud model allows unambiguous attribution of any observed discrepancies between bulk and explicit models to the nucleation and condensational growth processes. Based on previous studies with both explicit single-phase (Hegg and Hobbs, 1979), and bulk multi-phase models (Hegg et al., 1986), we hypothesize that these processes are the ones most likely to produce discrepancies between bulk and explicit models. The bulk-parameterized model utilizes the condensational growth algorithm of Yau and Austin (1979) and a chemical parameterization similar to that employed by Hegg et al. (1984).

The explicit microphysical model is essentially the same as that of Hegg and Hobbs (1979, 1986) and invokes the droplet growth expression of Fukuta and Walters (1970) which utilizes a condensation coefficient of 0.036 and an accommodation coefficient for water of 1.0. Because there is some sentiment in the cloud physics community for a higher value for the condensation coefficient, namely 1.0 (Mozurkewich, 1986; Leaitch et al., 1986), we have conducted a sensitivity study with the coefficient set to 1.0. The effect on our results was negligible. The equations for droplet growth and the various coupled continuity equations are integrated forward in time using a modified Adams technique. With the exception of the vertical velocity equation, which in our model is the kinematic profile mentioned above, these equations are the same as those in Pruppacher and Klett (1978). The model is initialized at 100% relative humidity at a pressure of 900 mb and a temperature of 0°C. Droplet growth commences on a pre-specified aerosol spectrum. The aerosol spectrum is divided into 75 different size classes, although the classes are defined in terms of activation supersaturation rather than size (the form and chemical composition of the spectrum is discussed below). The size range covered by the initial spectrum includes the lower accumulation and nucleation modes. It thus excludes the larger particles which play a negligible role in cloud chemistry because of their relatively negligible numbers. The width of each size class is variable but roughly 0.008 μm. A graph of this initial spectrum is given in Fig. 1. Because the droplet growth by condensation has a reciprocal dependence on the droplet radius, the droplet spectrum which forms on the activated aerosol tends to become monodisperse with time (see Fig. 1). This is characteristic of all such explicit models (e.g., Jensen and Charlson, 1984) and results in differ-

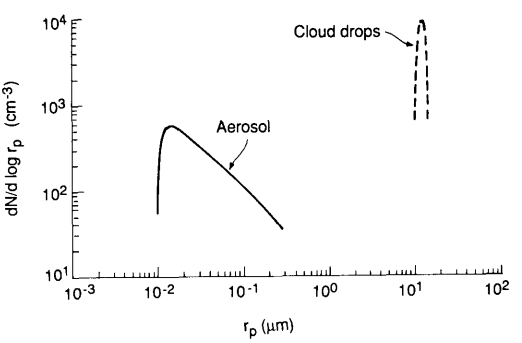

Fig. 1. The dry size distribution of the aerosol particles used as CCN, together with the droplet size spectrum formed on them after 465 s of model run time using the cumulus updraft.

ing concentrations of dissolved salts across the droplet spectrum due to the different initial masses of such salts across the initial aerosol spectrum.

On another issue, namely that of mass transport of reactants to and from the cloud water, some important differences between the two model types should be clarified. This is most easily discussed in terms of characteristic times. In the bulk model, the relevant characteristic times are associated with droplet growth, gas and liquid phase mass transport of trace species and chemical reactions within the drop. When these times are compared the usual conclusions are that liquid phase transport is rapid (Schwartz and Freiberg, 1981), and that gas phase transport is rapid for accommodation coefficients >0.01 (Chameides, 1984). Therefore, droplet growth and chemical reaction rates determine the overall characteristic time of the system and Henry's Law equilibrium is assumed between species in the gas and liquid phases.

The inclusion of an evolving droplet spectrum in the explicit model complicates the issue. Not only must the above rates be compared with each other for a given drop size, but these rates must also be compared across the droplet spectrum. While the assumption of Henry's Law equilibrium might be plausible for the less soluble species (O_3, SO_2) over the droplet sizes generated by the explicit model ($r < 14$ μm) according to both experimental (Walcek et al., 1984) and theoretical (Schwartz, 1986; Walcek and Pruppacher, 1984) studies, this assumption is not obviously appropriate for the highly soluble species (H_2O_2, NH_3). Therefore, in the explicit model we have allowed all gas-phase species to undergo explicit gas-phase mass transport. The transport rate is formulated in terms of the Fuchs-Sutugin transport equation (Fuchs and Sutugin, 1971) in the form:

$$\phi_i = (N_i - N_{is}) \int_0^r 4 D_i F A r N(r)\, dr$$

with

$$A = 1 + 1.333\,\mathrm{Kn}\,F(1/\alpha_i - 1) \qquad (1)$$

$$F = (1 + \mathrm{Kn})/(1 + 1.71\,\mathrm{Kn} + 1.333\,\mathrm{Kn}^2).$$

ϕ_i is the flux of the species i to the surface of a drop of radius r, D_i is the diffusion coefficient of the ith species through air, α_i is the accommodation coefficient for ith species on water drops, and N_i and N_{is} are the concentrations of the ith species in the far field and just above the drop surface, respectively. Kn is the Knudson number for the individual droplets. Following Chameides (1984), we employ the partial pressure predicted by Henry's Law, based on a given aqueous concentration of a drop, for the gas-phase concentration of a species just above the drop surface N_{is}. Several values of the accommodation coefficient, α_i, are utilized in the study.

The sulfate production reactions in both models will be oxidation of aqueous S(IV) by O_3, utilizing the rate expression of Maahs (1983), and by H_2O_2, utilizing the rate expression of Penkett et al. (1979). Utilizing the methodology of Schwartz and Freiberg (1981), for our study conditions the rate of physical mass transport within the droplet phase is rapid relative to the oxidation rate over almost all of the droplet spectrum and cloud water mass. We have therefore not included aqueous-phase mass transport rate expressions in the explicit microphysical model.

The initial aerosol in both models is assumed to be either $(NH_4)_2SO_4$ or NH_4HSO_4. Based on the studies of Weiss et al. (1982) and Tanner et al. (1984), most of the model simulations have been made with NH_4HSO_4. However, the study by Weiss et al. (1982), as well as numerous older studies (e.g., Charlson et al., 1974; Meszaros, 1978) indicate that $(NH_4)_2SO_4$ can sometimes dominate atmospheric sulfate and we have examined this composition in several model runs. The bulk concentration of sulfate for the base case is 0.8 μg m^{-3}.

For the explicit microphysical model, the sulfate is distributed over a cloud condensational nucleus (CCN) activation spectrum of the form: $\mathrm{CCN} = 290(\mathrm{ss})^{0.5}$ cm^{-3} where ss is the water vapor supersaturation (in %). This spectrum is typical of continental background—though not remote—air (Twomey and Wojciechowski, 1969). The concentration of drops for given cloud supersaturations predicted by this spectrum is given in Table 1. Several variations on this spectrum are employed in sensitivity studies. This spectrum, coupled with the assumed updraft profile, results in a nominal particle nucleation scavenging efficiency of 60–70% (depending on the updraft) and a sulfate mass scavenging efficiency

Table 1. *The concentration of drops activated at the given cloud supersaturations as predicted by the relationship: $N = 290\ (ss)^{0.5}$ (see text)*

Supersaturation (%)	No. drops/cm^3
0.04	58
0.12	100
0.20	130
0.28	153
0.34	169
0.42	188
0.50	205
0.58	221
0.66	236

of approximately 95%, similar to the value employed in the bulk model. The various gas-phase initial concentrations are presented in the discussion of model results.

Finally, because of the initially high ionic strengths of the unactivated aerosol particles (and even the activated aerosol particles during the first few seconds after activation) we have conducted sensitivity studies utilizing activities rather than concentrations for the sulfur and nitrogen species present in solution. For these calculations, values for the species activities in a single component system are derived from Young and Blatz (1949), and Goldberg and Parker (1985). These values are then applied to the mixed electrolytic solution of the droplets via the mixing rule of Kusik and Meissner (1978). In employing this rule, we neglect the presence of HSO_3^- and $SO_3^=$ (trace species) and also HSO_4^-, a more serious assumption. We thus assume that all sulfate is completely dissociated. The rationalization for this is that such an assumption overestimates the ionic strength of our solution droplets and thus yields lower limits on our activity coefficients. Therefore, if activity coefficients—as calculated—have no effect on our results, then more accurate calculations will also have no effect. We wish to emphasize that this approximation is utilized only in the activity coefficient calculations. All of these species are in fact present in the ion balance employed in the explicit model.

3. Initialization

For most of the variables included in the models, initialization proceeds in the conventional manner, i.e., initial concentrations of trace gases, a CCN activation spectrum in the explicit model and an aerosol particle mass in the bulk, and a kinematic flowfield are specific. The exception is the ammonium ion concentration in the particles which compose the initial CCN spectrum in the explicit model. The CCN are non-uniform, necessarily containing increasing amounts of sulfate as the activation supersaturation decreases. (Their initial sizes range from 0.05 to 1.0 μm radius at 100% relative humidity.) This, in turn, produces non-uniform acidity and consequently a non-uniform ammonium mass distribution over the CCN spectrum. The acidity and ammonium ion distributions are clearly interactive, with the unique NH_3 partial pressure at equilibrium with the various different NH_4^+ concentrations in the droplets requiring a numerical solution. The procedure employed in this study is to specify the initial sulfate distribution at 100% relative humidity and total moles of NH_3 and NH_4^+ per unit volume, calculate the completely unneutralized acidity (i.e., assume the sulfate is in the form of sulfuric acid), and then utilize the vapor/liquid mass transfer equations to iteratively titrate the sulfate until vapor-liquid equilibrium of ammonia is achieved across the droplet spectrum. In the course of this iterative procedure, necessary corrections to drop radii are made to maintain equilibrium with the water vapor field. We stress that this iterative approach is a technique to find the equilibrium partial pressure of NH_3. The actual physical assumption implicit in this technique is that equilibrium partitioning of NH_3 between gas and particles actually obtains prior to cloud formation, or that at least whatever partitioning does obtain is not perturbed except by cloud formation. This will certainly be true for most initial conditions. For example, we could have initialized the model at 95% relative humidity rather than 100% without changing our results in any significant way. The transition from 95% to 100% relative humidity prior to cloud formation simply does not perturb the initial NH_3–NH_4^+ distribution. It is also worth noting that the acid aerosol predominantly

utilized dictates quite low initial NH_3 partial pressures.

4. Results and discussion

All model runs were made out to 465 s. This time was selected both because the pH effects we shall deal with effectively disappear beyond this point (see Fig. 5) and because beyond this point collection processes will start to redistribute solute mass over the drop size distribution and render calculations very difficult (cf. Flossman et al., 1987). We thus note from the outset that we are dealing with a short-lived phenomenon.

Prior to assessing model differences in predictions of sulfate production, the bulk and explicit models were run without H_2O_2 and O_3 to examine differences in model predictions attributable to processes other than oxidation within cloud droplets (e.g., different condensational growth parameterizations). The results are shown in Table 2. We note first that the liquid water content of the explicit model is $\sim 18\%$ higher than that of the bulk model. This sort of discrepancy is attributable to the approximations implicit in the bulk parameterization and has been noted in many previous studies (e.g., Silverman and Glass, 1973). If the extent of dilution by condensational growth were the same in both models, then we would expect the explicit model to predict a lower value for cloud water sulfate than the bulk model. This is in fact the case although the sulfate concentration of the explicit formulation is $\sim 20\%$ lower than that of the bulk model, thus showing a very slight discrepancy from the relationship expected on the basis of the different liquid water contents of the two models. On the other hand, the pH of the bulk model is slightly higher than the volume weighted pH of the explicit model, just the opposite of what one would expect from dilution effects alone. This is due to the smaller CCN remaining unactivated in the explicit model. After activation and droplet growth, the ammonium ion is unevenly distributed over the CCN spectrum, being disproportionally present in the smaller, unactivated aerosol particles (see discussion of Fig. 2). For a fixed amount of total $NH_3 + NH_4^+$ per unit volume, the relatively higher concentration of ammonium in the smaller CCN effectively decreases the amount of ammonium ion available in the larger CCN, which do activate and form cloud water, and in the gas phase.

Table 2. *Values predicted by the bulk and explicit models for selected physical and chemical parameters after 465 seconds of run time*

Parameter	Bulk model	Explicit model
liquid water content[1]	1.28×10^{-3} g/g	1.5×10^{-3} g/g
temperature	269.43	269.6
height above cloud base	1053 m	1054 m
SO_2 concentration	0.13 ppb	0.15 ppb
bulk pH[2]	5.4	5.3
cloud water sulfate	4.44×10^{-6} M	3.56×10^{-6} M
H^+/NH_4^+	1.0	0.57–3.63[3] 0.25–0.3[4]

The gas-phase initial conditions were: $SO_2 = 0.2$ ppb, $O_3 = 0$ ppb, $NH_3 \simeq 2$ ppt, $H_2O_2 = 0$ ppb. The updraft used is the cumulus updraft.

[1] Liquid water contents at 465 s for the stratiform case are: bulk $= 3.2 \times 10^{-4}$ g/g, explicit $= 3.5 \times 10^{-4}$ g/g.

[2] In the explicit model, bulk pH is calculated by volume-weighted averaging over the droplet spectrum.

[3] Activated droplets.

[4] Unactivated droplets.

In both models, the initial ammonium concentration at cloud base in the droplets is at equilibrium with the gas-phase concentration. However, after activation and the commencement of droplet growth, equilibrium is no longer maintained in the explicit model. This situation is illustrated in Fig. 2, in which the ratio of actual to equilibrium ammonium concentration is plotted as a function of drop activation class at a simulation time of 465 s. For reference, the obvious result for the bulk equilibrium model, a horizontal line at a value of 1.0, is also plotted. The results shown here are for the cumulus updraft profile and for several different values of the NH_3 accommodation coefficient, as indicated. We note that the range of values for the accommodation coefficients (both for NH_3 and the other species) is that commonly assumed for this variable (cf. Chameides, 1984). Also, it is important to note that no S(IV) oxidation is present for

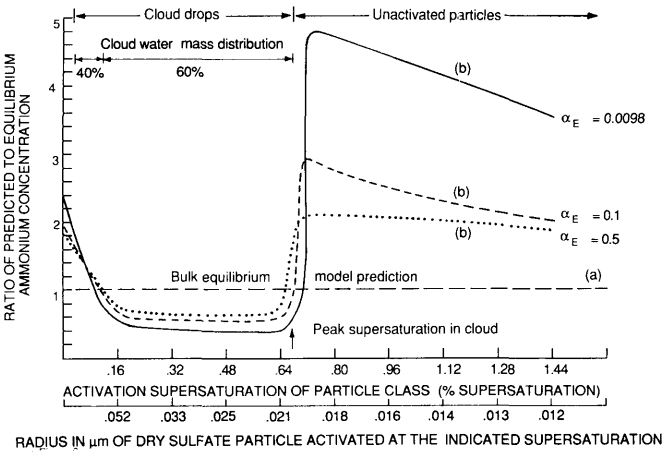

Fig. 2. The ratio of ammonium concentrations in a droplet to the concentrations predicted by Henry's Law as a function of droplet activation supersaturation with no S(IV) oxidation occurring. (a) The bulk equilibrium model, (b) the explicit model. The simulation time is 465 s. The discontinuity at a supersaturation of ca. 0.65% represents the peak supersaturation achieved in the simulation, i.e., particle classes to the right of this point are unactivated. The example here is for a cumulus updraft and NH_4HSO_4 aerosol. Results for several different accommodation coefficients are shown.

these cases. The form of the non-equilibrium distribution shown in Fig. 2 can be explained as follows. During the initial stages of droplet growth near cloud base, the largest CCN grow first, diluting rapidly. As a result of dilution, hydrogen ion is "produced" in these largest droplets due to the progressive ionization of bisulfate ion with decreasing solution strength. This tends to compensate for dilution of H^+ due to droplet growth, i.e., it "buffers" the H^+ concentration relative to dilution. Therefore, these largest droplets, with their larger water volume, have a reduced NH_3 vapor pressure at their surfaces relative to smaller CCN that have yet to activate. This causes transfer of NH_4^+ from these smaller CCN via the gas phase (i.e., NH_3) to the larger, activated droplets. However, droplet growth is sufficiently fast, and the growing droplets become sufficiently large, to preclude the attainment of gas-aqueous equilibrium. When the smaller CCN do finally activate and grow, the interstitial ammonia partial pressure and thus the driving forces for ammonia redistribution between drops has decreased significantly and the ammonium ion distribution across the droplet spectrum is essentially fixed over the remaining lifetime of the activated droplets. The supersaturation of the unactivated droplets with respect to NH_3 is also noteworthy. Although the smallest unactivated droplets ($\geq$0.65% activation saturation in Fig. 2) have actually lost NH_4^+ to the activated drops, they have not lost it at a rate comparable to the rate of depletion of interstitial NH_3. This is due to their very high acidity ($pH \leq 1$), which results in a very low NH_3 equilibrium vapor pressure over their surfaces, and their small size and consequent high Knudson numbers. Both of these effects will greatly reduce mass transport from the droplets to the gas phase (see eq. (1)). Incidentally, this small size is the reason for the importance of the accommodation coefficient as shown in Fig. 2. Of course, this skewed distribution of ammonium across the droplet spectrum also results in a skewed hydrogen ion distribution.

Interestingly, the skewed distribution of ammonium and hydrogen ions across the droplet spectrum predicted by the explicit model has been observed in field studies. For example, Daum et al. (1984a) in a study of the chemical composition of stratiform clouds, noted that the bulk ratio of H^+ to NH_4^+ in their cloud water samples was always higher than the same ratio in unactivated (interstitial) haze particles measured

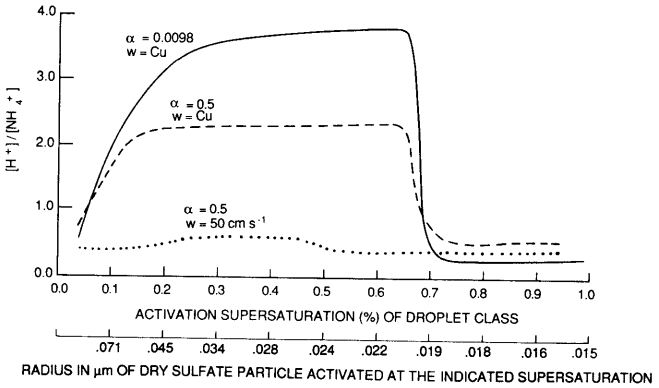

Fig. 3. The variation across the droplet spectrum of the ratio of $[H^+]$ to $[NH_4^+]$. Several different model runs are shown to illustrate the effects of initial conditions on the distribution.

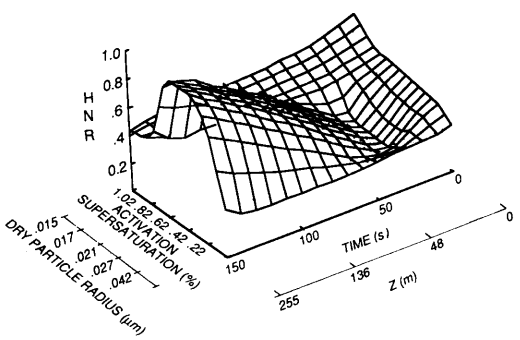

Fig. 4. A plot of the dependence of the ratio of hydrogen ion to ammonium ion (HNR) on both droplet activation supersaturation and time. The time axis is reversed to highlight the magnitude of the dichotomy between activated and unactivated droplets. The case shown is that for the middle curve of Fig. 3. Also shown is the height above cloud base which corresponds to the time scale.

roughly simultaneously. The H^+/NH_4^+ ratio in the cloud water ranged from 1.9 to >35 (with most values between 2 and 8), whereas the ratio in the interstitial particles, when measurable, ranged from <0 (net basicity after blank correction in Gran titration) to 0.9. Measurement of out-of-cloud particle composition revealed bulk ratios similar to the interstitial bulk ratios. Earlier, though less complete, measurements of the same sort were obtained by Lazrus et al. (1983). In comparison, values for the H^+/NH_4^+ ratio predicted by the explicit model for the run specified in Table 2 range from 0.57 to 3.63 for the activated drops (cloud water), 0.2 to 0.3 for the unactivated (interstitial) particles, and by definition, 1.0 for the pre-cloud (out-of-cloud) bulk ratio. The variation in H^+/NH_4^+ across the droplet spectrum predicted by the model is shown graphically in Fig. 3 for several different initial conditions and a simulation time of 465 s. The time evolution of this effect is shown in Fig. 4 for the case of the middle curve shown in Fig. 3. It is important to note that this variability in time will produce a concurrent variability in space since the model is one-dimensional. To illustrate this, the height above cloud base is also displayed in Fig. 4. Quite clearly the skewed ammonium distribution predicted by the explicit model is consistent with the observations of Daum et al. (1984a). However, the preferred explanation for their results of both Daum et al. and Lazrus et al. was, in part, sulfate production in solution, although Daum et al. point out that their data set does not preclude other explanations (e.g., sampling artifacts). They rejected an alternative explanation of selective activation of acidic aerosol particles because, in the words of Daum et al., "selective activation of an acidic aerosol particle in preference to its ammonium salt seems unlikely". Furthermore, in a more extensive study, Daum et al. (1984b) found the contrast in composition between cloud water and either out-of-cloud or interstitial particles to be ubiquitous.

Table 3. *Predictions of sulfate production by the bulk and explicit models for various initial conditions*

Case					Sulfate production			Explicit production due to O_3 (%)
SO_2 (ppbv)	H_2O_2 (ppbv)	α_ε	Initial aerosol $NH_4^+/SO_4^=$	Updraft (cm S^{-1})	Bulk model (g/g air)	Explicit model (g/g air)	Ratio explicit bulk	
0.2	1.0	0.5	1	cumulus	3.8×10^{-10}	6.3×10^{-10}	1.7	82
0.2	0.5	0.5	1	cumulus	2.8×10^{-10}	5.8×10^{-10}	2.1	90
0.2	0	0.5	1	cumulus	1.7×10^{-10}	5.2×10^{-10}	3.1	100
0.2	0.5	0.0098	1	cumulus	2.8×10^{-10}	5.6×10^{-10}	2.0	
0.2	0	0.0098	1	cumulus	1.7×10^{-10}	5.0×10^{-10}	2.9	
0.2	0.5	0.5	1	50	1.6×10^{-10}	2.0×10^{-10}	1.3	74
0.2	0.1	0.5	1	50	4.4×10^{-11}	1.4×10^{-10}	3.2	94
0.2	0	0.5	1	50	6.0×10^{-12}	1.3×10^{-10}	21.7	100
0.2	0.5	0.0098	1	50	1.6×10^{-10}	1.8×10^{-10}	1.1	
0.2	0	0.0098	1	50	6.0×10^{-12}	1.2×10^{-10}	20.0	
0.2	0.5	0.5	2	50	2.0×10^{-12}	2.4×10^{-12}	1.2	
2.0	0.5	0.5	1	cumulus	2.4×10^{-9}	1.8×10^{-9}	0.8	57
2.0	0	0.5	1	cumulus	3.5×10^{-10}	1.3×10^{-9}	3.7	100
2.0	0.5	0.5	1	50	8.5×10^{-10}	8.0×10^{-10}	0.9	27
2.0	0	0.5	1	50	8.4×10^{-12}	2.6×10^{-10}	30.9	100
2.0	0.5	0.5	2	50	8.7×10^{-10}	8.4×10^{-10}	1.0	
2.0	0	0.5	2	50	1.6×10^{-11}	3.3×10^{-10}	20.6	

Simulation time = 465. O_3 = 50 ppb, CCN = 290 $(ss)^{0.5}$ cm^{-3}.

In our view, this is more in accord with an explanation based on nucleation, which is ubiquitous, than on sulfate production, which does not occur at measurable levels this commonly (cf. Hegg and Hobbs, 1982, 1986). Indeed, the data of Daum et al. (1984a) show no evidence of sulfate production based on a sulfate mass balance. On the other hand, the model results indicate that H^+/NH_4^+ ratios in activated droplets much in excess of ~ 4 cannot be explained by the non-equilibrium NH_3-acidity partitioning just discussed and that they can be easily obtained with modest sulfate production. Furthermore, elevated H^+/NH_4^+ ratios in activated droplets are clearly dependent on the as yet poorly known accommodation coefficient for NH_3 and the vertical velocity in the cloud. Thus, the earlier field studies cited above may well display some evidence of sulfate production. Nevertheless, it seems clear to us that assertions of sulfate production based primarily on differences in the acidity of cloud water and pre-cloud particles should be reassessed.

A comparison of predictions of sulfate production by the bulk and explicit models for various initial conditions is shown in Table 3. These results show several interesting features. First, the differences between the predictions of the bulk and explicit models can range up to a factor of 31 (though factors of 2 and 3 are typical), with the explicit model generally predicting more sulfate production than the bulk model. The differences between the models tend to increase with decreasing H_2O_2 concentrations. For H_2O_2 concentrations of 1 ppb or greater, the bulk versus explicit model predictions will not differ greatly (a factor of 1.65 or less). For the higher SO_2 concentrations (2 ppb) the models differ appreciably less than at lower SO_2 concentrations. The effect of H_2O_2 is easily rationalized. The H_2O_2 oxidation reaction has a negligible pH dependence and would therefore render inhomogeneities in droplet pH across the droplet spectrum—the major difference between the explicit and bulk formulations—of little significance if it were the dominant S(IV) oxidant. The expla-

nation for the effects of SO_2 is somewhat more involved. In the case of the higher SO_2 values, the amount of sulfate produced in the cloud droplets is comparable to the initial sulfate in the droplets and thus can significantly alter droplet pH. Since the sulfate will be produced preferentially in the higher pH droplets, the production itself will "homogenize" the droplet pH's and thus reduce differences in sulfate production between the bulk and explicit models. For the lower SO_2 concentrations, the sulfate produced in the droplets is a relatively modest fraction of the initial sulfate and thus has a correspondingly modest effect on droplet pH. Differences in pH across the droplet spectrum will therefore tend to persist, allowing more sulfate production in the higher pH droplets. Hence, the discrepancy between models is larger at low SO_2 and/or oxidant values. An example of the difference in pH across the droplet spectrum, for a model run with low SO_2, is shown in Fig. 5. However, it is important to note that even for this low SO_2 case, the sulfate production reaction itself tends to "homogenize" cloud droplet sulfate concentrations with time (or distance above cloud base). This effect will, of course, be absent when sulfate production does not take place, as can be seen from the studies of Jensen and Charlson (1984) and Twohy et al. (1989).

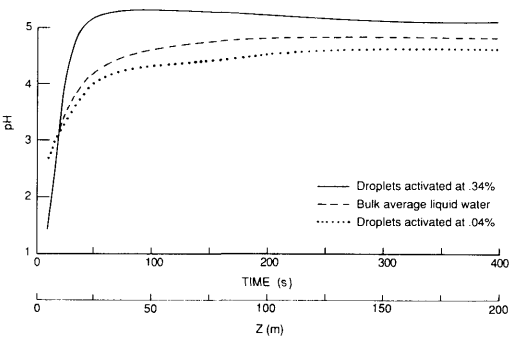

Fig. 5. The pH of a droplet as a function of time and height above cloud base for two different activation classes (activation supersaturations of 0.04 and 0.34%), and the bulk liquid water content. Initial conditions of: $SO_2 = 0.2$ ppb. $O_3 = 50$ ppb, $H_2O_2 = 0.1$ ppb, NH_4HSO_4 CCN. The updraft was a constant 50 cm s^{-1}.

Another facet of the time or space variation of chemical concentrations just mentioned is the change in chemical concentrations with height in cloud. Plots of in-cloud concentrations of SO_2, H_2O_2 and particulate $SO_4^=$ against height above cloud base are shown in Fig. 6 for the cumulus profile. The SO_2 and H_2O_2 concentrations are, of course, interstitial whereas the $SO_4^=$ concentration is the equivalent partial pressure of aqueous sulfate (interstitial $SO_4^=$ is negligible). The concentrations shown are in general agreement with observations (e.g., Kelly et al., 1985; Bath et al., 1989) and the trend shown is also in agreement with limited observations (Leaitch et al., 1983).

One other point of some interest, which is illustrated in Table 3, is the importance of ozone oxidation. On the basis of bulk pH, one would not expect O_3 to play a particularly significant

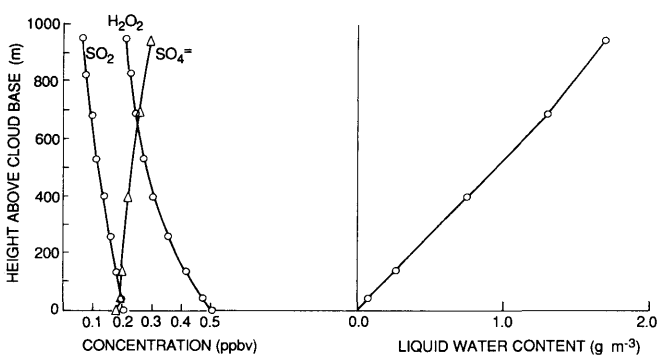

Fig. 6. Vertical profiles of SO_2, H_2O_2, and aqueous $SO_4^=$ predicted by the model using the cumulus updraft. The height axis is the height above cloud base.

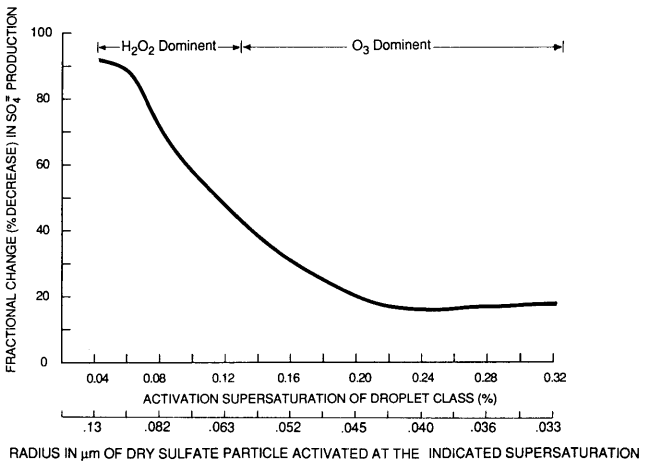

Fig. 7. Fractional decrease in sulfate production in each droplet class due to decreasing initial H_2O_2 from 0.5 ppb to 0. The base case has 0.2 ppb SO_2, 50 ppb O_3.

role in sulfate production. However, the last column of Table 3, which shows the percentage of sulfate produced in the explicit model (for a range of cases) which is due to O_3, suggests otherwise. For the low SO_2 cases, O_3 is actually the dominant oxidant. Even for the high SO_2 cases, it has a significant role. Clearly, the higher pH droplets in the explicit model provide a favorable medium for ozone oxidation of aqueous S(IV). The plot in Fig. 7 indicates that sulfate production is decreasingly sensitive to H_2O_2 concentrations as the droplet activation supersaturation (and thus droplet pH) increases. Nevertheless, if H_2O_2 is present, it will preferentially oxidize some of the S(IV) which would otherwise be oxidized by O_3, at least in the lower pH drops. It is not clear, except in extreme circumstances, which oxidant is "dominant". The results shown here simply point out that O_3 oxidation can be of great importance when the model bulk pH would suggest otherwise and augment the arguments of Perdue and Beck (1988) with regard to the caution necessary when interpreting bulk cloud water measurements.

These results, when coupled with recent field measurements of SO_2 and H_2O_2 in the Eastern and Central United States (e.g., Heikes et al., 1987; Van Valin et al., 1987; Barth et al., 1989), suggest that bulk-parameterized models will adequately predict sulfate production in such areas during the summer months. At lower SO_2 concentrations, typical of remote locations (Maroulis et al., 1980; Georgii and Meixner, 1980), the situation is less clear cut. Certainly during the winter months when H_2O_2 concentrations are also relatively low (commonly less than 0.5 ppb) the results presented here suggest that bulk-parameterized models can significantly, indeed sometimes drastically, underpredict sulfate production.

The effect of the accommodation coefficient for the various trace gases on sulfate production is also apparent in Table 3. Most such evaluations were made with initial conditions of 50 ppb O_3, an initial CCN composition of NH_4HSO_4, and 0.2 ppb SO_2. With regard to sulfate production, only a rather minor effect ($\leqslant 4\%$) is apparent. It acts through altering the NH_4^+ distribution across the droplet spectrum rather than through transport limitation of reactants (neither aqueous S(IV) nor H_2O_2 depart from their Henry's Law equilibrium values by more than 2%). Similarly, inclusion of activity coefficients in the model to more realistically deal with liquid-vapor partitioning and various aqueous dissociation reactions produced a negligible effect ($<4\%$). While somewhat surprising, this latter lack of sensitivity is readily explicable.

The initial aerosol is sufficiently acidic that virtually all of the ammonia is in the aqueous phase whether one utilizes concentrations or activities; i.e., the inclusion of activity coefficients only minimally changes aqueous NH_4^+ (though it does significantly lower gas-phase NH_3). Similarly, most of the SO_2 is initially in the gas-phase, whether activities are involved or not. Furthermore, in this case the aqueous response of the system to higher SO_2 solubility is partially damped by the various aqueous SO_2 equilibria. After droplet activation, the effects of the activity coefficient are minimized by the very rapid decrease in ionic strength of the droplets as they grow.

Finally, several model runs were made to evaluate the influence of the CCN spectrum on sulfate production. This influence appears to be modest. For example, a spectrum of the form $CCN = 1028\ (ss)^{1.0}\ cm^{-3}$ (typical of moderately polluted air) produces only a $\sim 9\%$ increase in sulfate production over the standard spectrum [$CCN = 290\ (ss)^{0.5}\ cm^{-3}$]. Incidentally, a change in the CCN spectrum has a somewhat more marked influence on the H^+/NH_4^+ ratio across the droplet spectrum. For example, the spectrum just discussed increased the H^+/NH_4^+ ratio in the activated droplets by a factor of ~ 1.5 over the standard case.

It would be of interest to examine in more detail the effect of SO_2 partial pressure and H_2O_2 level on the distribution of sulfate production across the droplet spectrum. In addition, the behavior of soluble acid vapors that initially are predominantly in the gas phase (for example, HNO_3) should also be examined.

5. Conclusions

The model results presented here suggest that bulk-parameterized cloud chemistry models will adequately predict total sulfate production in clouds under conditions of high SO_2 ($\geqslant 2$ ppb) and high H_2O_2 ($\geqslant 0.5$ ppb). The potential errors will be largest (up to a factor of 30) under conditions of low SO_2 ($\leqslant 2.0$ ppb) and low H_2O_2 ($\leqslant 0.5$ ppb). The major source of error in the bulk model under these conditions is the assumption that droplet pH does not vary with droplet size. Predictions of sulfate production are in error because droplet pH varies across the droplet size spectrum, a consequence of size dependent sulfate and ammonium distributions, and renders bulk cloud water pH a parameter which is not always representative of reaction conditions. Related to this, the ozone oxidation of aqueous S(IV) appears to be of more significance than would be suggested by bulk pH measurements. Furthermore, literature values of the relative acidity of activated versus unactivated CCN are consistent with the predictions of the explicit microphysical model and suggest that great care be exercised when basing assertions of sulfate production on elevated ratios of $[H^+]/[NH_4^+]$ in cloud droplets. Finally, the CCN used in this study are chemically homogeneous, i.e., they constitute an internal mixture. However, preliminary calculations by Twohy et al. (1989) suggest that commonly occurring externally mixed aerosols—such as marine aerosols—can produce an even more drastic variation of pH across the droplet spectrum formed by their activation. Studies of SO_2 oxidation in clouds formed on such aerosols should be undertaken.

6. Acknowledgements

We wish to acknowledge partial support of this research by Grant RP 1630-45 from the Electric Power Research Institute and by Grants ATM-8419000 and ATM-8715892 from the National Science Foundation.

REFERENCES

Barth, M. C., Hegg, D. A., Hobbs, P. V., Walega, J. G., Kok, G. L., Heikes, B. G. and Lazrus, A. L. 1989. Measurements of atmospheric gas-phase and aqueous-phase hydrogen peroxide concentrations in winter on the East Coast of the United States. *Tellus 41B*, 61–69.

Chameides, W. L. 1984. The photochemistry of a remote marine stratiform cloud. *J. Geophys. Res. 89*, 4739–4756.

Charlson, R. J., Vanderpol, A. H., Covert, D. S., Waggoner, A. P. and Ahlquist, N. C. 1974. Sulfuric acid-ammonium sulfate aerosol: optical detection in the St. Louis region. *Science 184*, 165–168.

Daum, P. H., Schwartz, S. E. and Newman, L. 1984a.

Acidic and related constituents in liquid water stratiform clouds. *J. Geophys. Res. 89*, 1447–1458.

Daum, P. H., Kelly, T. J., Schwartz, S. E. and Newman, L. 1984b. Measurements of chemical composition of stratiform clouds. *Atmos. Environ. 18*, 2671–2684.

Easter, R. C. and Hales, J. M. 1983. Interpretation of the OSCAR data for reactive gas scavenging. In: *Precipitation Scavenging, Dry Deposition and Resuspension* (eds. H. R. Pruppacher, R. G. Semonin and W. G. Slinn). Elsevier, New York, 649–662.

Flossman, A. I., Hall, W. D. and Pruppacher, H. R. 1985. A theoretical study of the wet removal of atmospheric pollutants. Part I: The redistribution of aerosol particles captured through nucleation and impaction scavenging by growing cloud drops. *J. Atmos. Sci. 42*, 583–606.

Flossman, A. I., Pruppacher, H. R. and Topalian, J. H. 1987. A theoretical study of the wet removal of atmospheric pollutants. Part II: The uptake and redistribution of $(NH_4)_2SO_4$ particles and SO_2 gas simultaneously scavenged by growing cloud drops. *J. Atmos. Sci. 44*, 2912–2923.

Fuchs, N. A. and Sutugin, A. G. 1970. *Highly dispersed aerosols.* Ann Arbor Science Publisher, Ann Arbor, MI., pp. 105.

Fukuta, N. and Walters, L. A. 1970. Kinetics of hydrometeor growth from a vapor spherical model. *J. Atmos. Sci. 27*, 1160–1172.

Georgii, H. W. and Meixner, F. X. 1980. Measurement of the tropospheric and stratospheric SO_2 distribution. *J. Geophys. Res. 85*, 7433–7438.

Goldberg, C. L. and Parker, N. 1985. Review of activities of sulfur species in solution. *J. Res. Nat. Bur. Stds. 90*, 341–358.

Hegg, D. A., and Hobbs, P. V. 1979. The homogeneous oxidation of SO_2 in cloud drops. *Atmos. Environ. 13*, 981–987.

Hegg, D.A., and Hobbs, P. V. 1982. Measurements of sulfate production in natural clouds. *Atmos. Environ. 16*, 2663–2668.

Hegg, D. A. and Hobbs, P. V. 1986. Sulfate and nitrate chemistry in cumuliform clouds. *Atmos. Environ. 20*, 901–909.

Hegg, D. A., Rutledge, S. A. and Hobbs, P. V. 1984. A numerical model for sulfur chemistry in warm-frontal rainbands. *J. Geophys. Res. 89*, 7133–7149.

Hegg, D. A., Rutledge, S. A. and Hobbs, P. V. 1986. A numerical model of sulfur and nitrogen scavenging in narrow cold frontal rainbands. II. Discussion of chemical fields. *J. Geophys. Res. 91*, 14404–14416.

Heikes, B. G., Kok, G. L., Lazrus, A. L. and Walega, J. G. 1987. H_2O_2, O_3 and SO_2 measurements in the lower troposphere over the eastern USA during fall. *J. Geophys. Res. 92*, 915–932.

Hong, M. S. and Carmichael, G. R. 1983. An investigation of sulfate production in clouds using a flow-through chemical reactor model approach. *J. Geophys. Res. 88*, 10733–10743.

Howell, W. E. 1949. The growth of cloud drops in uniformly cooled air. *J. Met. 6*, 134–145.

Hough, A. M. 1987. A computer modeling study of the chemistry occurring during cloud formation over hills. *Atmos. Environ. 21*, 1073–1095.

Jacob, D. J. and Hoffman, M. R. 1983. A dynamic model for the production of H^+, NO_3^-, and $SO_4^=$ in urban fog. *J. Geophys. Res. 88*, 6611–6621.

Jensen, J. B., and Charlson, R. J. 1984. On the efficiency of nucleation scavenging. *Tellus 36B*, 267–375.

Kelly, T. J., Daum, P. H. and Schwartz, S. E. 1985. Measurements of peroxides in cloudwater and rain. *J. Geophys. Res. 90*, 7861–7871.

Kusik, C. L. and Meissner, H. D. 1978. Electrolytic activity coefficients in inorganic processing. *A. I. Ch. E. Symp. Ser. 173*, 14–20.

Lazrus, A. L., Haagenson, P. L., Kok, G. L., Huebert, D. J., Kreitzberg, C. W., Likens, G. E., Mohnen, V. A., Wilson, W. E. and Winchester, J. W. 1983: Acidity in air and water in the case of warm-frontal precipitation. *Atmos. Environ. 17*, 581–592.

Leaitch, W. R., Strapp, J. W., Wiebe, H. A. and Isaac, G. A. 1983. Measurements of scavenging and transformation of aerosol inside cumulus. In: *Precipitation scavenging, dry deposition and resuspension* (eds. H. R. Pruppacher, R. G. Semonin and W. G. Slinn). Elsevier, New York, 53–66.

Leaitch, W. R., Strapp, H. A., Isaac, G. A. and Hudson, J. G. 1986. Cloud droplet nucleation and cloud scavenging of aerosol sulphate in polluted atmospheres. *Tellus 38B*, 328–344.

Lee, L. Y. and Shannon, J. D. 1985. Indications of nonlinearities in processes of wet deposition. *Atmos. Environ. 19*, 143–150.

Maahs, H. G., 1983. Measurements of the oxidation rate of sulfur (IV) by ozone in aqueous solution and their relevance to SO_2 conversion in non-urban tropospheric clouds. *Atmos. Environ. 17*, 341–346.

Maroulis, P. J., Torres, A. L., Goldberg, A. B. and Bandy, A. R. 1980. Atmospheric SO_2 measurements on project game tag. *J. Geophys. Res. 85*, 7345–7349.

Mason, B. J. and Chien, C. W. 1962. Cloud-droplet growth by condensation in cumulus. *Q. J. R. Met. Soc. 88*, 133–138.

Meszaros, A., 1978. On the concentration and size distribution of atmospheric sulfate particles under rural conditions. *Atmos. Environ. 12*, 2425–2428.

Mozurkewich, M. 1986. Aerosol growth and the condensation coefficient. *Aerosol Sci. & Tech. 5*, 223–236.

Noone, K. J., Charlson, R. J., Covert, D. S., Ogren, J. A. and Heintzenberg, J. 1988. Cloud droplets: Solute concentration is size dependent. *J. Geophys. Res. 93*, 9477–9482.

NRC, 1984. *Global tropospheric chemistry, a plan for action.* National Academy Press, Washington, DC.

Penkett, S. A., Jones, B. M., Brice, A. and Eggleton, A. E. 1979. The importance of atmospheric ozone

and hydrogen peroxide in oxidizing sulfur dioxide in clouds and rainwater. *Atmos. Environ. 13*, 123–127.

Perdue, E. M. and Beck, K. C., 1988. Chemical consequences of mixing atmospheric droplets of varied pH. *J. Geophys. Res. 93*, 691–698.

Schwartz, S. E., 1986. Mass-transport considerations pertinent to aqueous phase reactions of gases in liquid-water clouds. In: *Chemistry of multiphase atmospheric systems* (ed. W. Jaeschke). Springer-Verlag, Berlin, 415–471.

Schwartz, S. E. and Freiberg, J. E. 1981. Mass-transport limitation to the rate of reaction of gases in liquid droplets: application to oxidation of SO_2 in aqueous solutions. *Atmos. Environ. 15*, 1129–1144.

Silverman, B. A. and Glass, M. 1973. A numerical simulation of warm cumulus clouds: Part 1. Parameterized vs. non-parameterized microphysics. *J. Atmos. Sci. 30*, 1620–1637.

Tanner, R. L., Kumer, R. and Johnson, S. 1984. Vertical distribution of aerosol strong acid and sulfate in the atmosphere. *J. Geophys. Res. 89*, 7149–7158.

Trembley, A. and Leighton, H. 1984. The influence of cloud dynamics upon the redistribution and transformation of atmospheric SO_2—a numerical simulation. *Atmos. Environ. 18*, 1885–1894.

Twohy, C. H., Austin, P. H. and Charlson, R. J. 1989. Chemical consequences of the initial diffusional growth of cloud droplets: a clean marine case. *Tellus 41B*, 51–60.

Twomey, S. and Wojciechowski, T. A. 1969. Observations of the geographical variation of cloud nuclei. *J. Atmos. Sci. 26*, 684–688.

Van Valin, C. C., Ray, J. D., Boatman, J. F. and Gunter, R. L. 1987. Hydrogen peroxide in air during winter over the central United States. *Geophys. Res. Letts. 14*, 1146–1149.

Venkatram, A. and Karamchandari, P. 1986. Source-receptor relationships, a look at acid deposition modeling. *Environ. Sci. and Technol. 20*, 1084–1091.

Walcek, C. J. and. Pruppacher, H. R. 1984. On the scavenging of SO_2 by cloud and raindrops. I: A theoretical study of SO_2 absorption and desorption for water drops in air. *J. Atmos. Chem. 1*, 269–289.

Walcek, C. J., Pruppacher, H. R., Topalian, J. H. and Mitra, S. K. 1984. On the scavenging of SO_2 by cloud and raindrops. II: An experimental study of SO_2 absorption and desorption for water drops in air. *J. Atmos. Chem. 1*, 291–306.

Weiss, R. E., Larson, T. V. and Waggoner, A. P. 1982. In situ rapid-response measurements of H_2SO_4/$(NH_4)_2SO_4$ aerosols in rural Virginia. *Environ. Sci. and Technol. 16*, 525–532.

Yau, M. K. and Austin, P. M. 1979. A model for hydrometeor growth and evolution of raindrop size spectra in cumulus cells. *J. Atmos. Sci. 36*, 655–668.

Young, T. F. and Blatz, L. A. 1949. The variation of the properties of electrolytic solutions with degrees of disassociation. *Chem Rev. 44*, 93–115.